



Solar System evolution and terrestrial planet accretion determined by Zr isotopic signatures of meteorites



Jan Render^{a,b,*}, Gregory A. Brennecka^b, Christoph Burkhardt^a, Thorsten Kleine^{a,c}

^a Institut für Planetologie, University of Münster, Wilhelm-Klemm-Straße 10, Münster, 48149 Germany

^b Nuclear and Chemical Sciences Division, Lawrence Livermore National Laboratory, 7000 East Ave., Livermore, CA, USA

^c Max Planck Institute for Solar System Research, Justus-von-Liebig-Weg 3, 37077 Göttingen, Germany

ARTICLE INFO

Article history:

Received 4 April 2022

Received in revised form 21 July 2022

Accepted 22 July 2022

Available online 17 August 2022

Editor: F. Moynier

Keywords:

zirconium

nucleosynthetic anomalies

early Solar System

accretion

ABSTRACT

Nucleosynthetic isotope signatures in meteorites provide key insights into the structure and dynamics of the solar protoplanetary disk and the accretion history of the planets. We present high-precision Zr isotopic data of a comprehensive suite of non-carbonaceous (NC) and carbonaceous (CC) meteorites, and find that various meteorite groups, including enstatite chondrites, exhibit ⁹⁶Zr enrichments, whereas there is no resolved ⁹¹Zr and ⁹²Zr variability. These new Zr isotope data reveal the same fundamental NC-CC dichotomy observed for several other elements, where CC meteorites are more anomalous compared to NC meteorites and are shifted towards the isotopic composition of Ca-Al-rich inclusions (CAIs). For Zr and other elements, the CC composition is reproduced as a mixture of materials with CAI-like and NC-like isotopic compositions in approximately constant proportions, despite these elements exhibiting disparate nucleosynthetic origins or different cosmo- and geochemical behaviors. These constant mixing proportions are inconsistent with an origin of the dichotomy by thermal processing or selective dust-sorting in the disk but indicate mixing of isotopically distinct materials with broadly solar chemical compositions. This corroborates models in which the NC-CC dichotomy reflects time-varied infall from an isotopically heterogeneous molecular cloud. Among NC meteorites, the isotope anomalies in Zr are linearly correlated with those of other elements, which likewise reflects primordial mixing. Lastly, the new Zr isotope data reinforce the notion that Earth incorporated s-process enriched material from the innermost Solar System, which is not represented by known meteorites. By contrast, contributions to Earth and Mars from outer Solar System CC-like materials were limited, indicating that these planets did not form by pebble accretion, which would have led to high CC fractions.

© 2022 The Author(s). Published by Elsevier B.V. This is an open access article under the CC BY-NC-ND license (<http://creativecommons.org/licenses/by-nc-nd/4.0/>).

1. Introduction

Nucleosynthetic isotope variations among meteorites and planets result from the heterogeneous distribution of isotopically anomalous presolar material in the solar accretion disk. The exact mechanism responsible for establishing this isotopic heterogeneity is debated, and selective thermal processing or size-sorting of presolar materials in the disk (e.g., Trinquier et al., 2009; Burkhardt et al., 2011; Steele et al., 2012), changes in the composition of infalling molecular cloud material (Nanne et al., 2019; Burkhardt et al., 2019; Jacquet et al., 2019), or a combination thereof (Ek et al., 2020) have been proposed. Regardless of their cause, nucleosynthetic isotope variations in meteorites have proven highly benefi-

cial for establishing genetic links among and between meteorites and planets. For example, bulk meteorites exhibit a fundamental isotopic dichotomy between non-carbonaceous (NC) and carbonaceous (CC) meteorites, indicating that meteorite parent bodies formed in two spatially separated, but coexisting disk reservoirs. Within this framework, the NC reservoir is commonly associated with the inner Solar System, whereas the CC reservoir may represent the outer Solar System beyond the orbit of Jupiter (Warren, 2011; Kruijer et al., 2017; Morbidelli et al., 2022).

A promising element for further study of the nucleosynthetic heterogeneity of the early Solar System is zirconium (Zr). As a refractory lithophile element, Zr is neither affected by volatile loss processes nor by core formation, meaning that the entire Zr inventory of a differentiated parent body is present in its silicate mantle. Moreover, Zr is almost entirely unaffected by cosmic ray induced neutron-capture or spallation processes, rendering any isotopic effects from irradiation by galactic cosmic rays negligible at the current analytical precision (Leya et al., 2003). As such, the Zr isotopic

* Corresponding author at: Nuclear and Chemical Sciences Division, Lawrence Livermore National Laboratory, 7000 East Ave., Livermore, CA 94450, USA.

E-mail address: render1@llnl.gov (J. Render).

composition of bulk silicate Earth (BSE), bulk silicate Mars (BSM), and the silicate mantles of other Solar System bodies represent an integrated average over their entire accretion history and allow for determining the nature and origin of a planet's bulk building material. In particular, relating the Zr isotopic signatures of NC and CC meteorites to those of the BSE and BSM can provide information on the nature and origin of the building blocks and, ultimately, the formation mechanism of the terrestrial planets (Dauphas, 2017; Burkhardt et al., 2021).

Zirconium consists of five stable isotopes (^{90}Zr , ^{91}Zr , ^{92}Zr , ^{94}Zr , and ^{96}Zr). Of those, ^{91}Zr typically shows no or only very small anomalies (e.g., Schönbächler et al., 2005; Akram et al., 2015; Elfers et al., 2020), and ^{92}Zr can host radiogenic ingrowth from ^{92}Nb (Iizuka et al., 2016; Haba et al., 2021), such that the anomalies in the neutron-rich ^{96}Zr are the most diagnostic when the commonly employed internal normalization to $^{94}\text{Zr}/^{90}\text{Zr}$ is used (for a more in-depth explanation of Zr nucleosynthesis, we refer to Akram et al., 2013). Zirconium isotope heterogeneity has been shown for chemical separates of carbonaceous chondrites (Schönbächler et al., 2005; Elfers et al., 2020), Ca-Al-rich inclusions (Akram et al., 2013), and some bulk carbonaceous chondrites (Akram et al., 2015). However, unlike the nucleosynthetic isotope anomalies for other elements, there does not seem to be a clear distinction between NC and CC meteorites in Zr isotopes, and their ^{96}Zr signatures seem to partially overlap (Akram et al., 2015). Moreover, high-precision Zr isotope data are missing for many NC meteorites, with the exception of the recently reported anomalies in eucrites and angrites (Render and Brennecka, 2021) and Zr isotope data for Mars (Burkhardt et al., 2021). Hence, the collective Zr isotope dataset is so far incomplete and systematic Zr isotopic anomalies within the suite of NC meteorites have not yet been demonstrated. To assess whether NC meteorites exhibit systematic Zr isotope anomalies, and how these relate to the composition of the CC reservoir, Earth, and Mars, we present new high-precision Zr isotope data for a range of NC and CC meteorites, many of them not previously measured for Zr isotopes. The new data are used to assess whether there is an NC-CC dichotomy for Zr, to unravel the origin of Zr isotope variations among meteorites, and to constrain the origin and nature of the building blocks of the terrestrial planets.

2. Samples and methods

2.1. Samples

The samples of this study include a representative set of chondritic and differentiated meteorites from both the NC and the CC suites, most of which have previously been digested and chemically processed for Mo (Burkhardt et al., 2011; Budde et al., 2019), Ru (Hopp et al., 2020), and U (Goldmann et al., 2015) investigations. As such, one strength of the present dataset is the possibility of detailed comparisons of isotopic signatures in different elements from the same sample digestions (Table S2 in the supplementary information lists the elements investigated for each sample as well as the associated references). For several meteorite groups we report the first Zr isotope data: Rumuruti, Kakangari, CH, and CL chondrites, winonaites, acapulcoites, mesosiderites, and main-group (MG) pallasites, as well as three ungrouped achondrites from the NC and CC reservoirs (Table 1). This comprehensive sample set, together with the Zr isotope data for angrites, eucrites, and martian meteorites published previously (Render and Brennecka, 2021; Burkhardt et al., 2021), allows for the thorough assessment of any Zr isotope variations among NC meteorites and for identifying the differences between NC meteorites and Earth.

In addition, we also analyzed acid leachates from a sequential dissolution of ~ 16.5 g whole-rock powder of the CM2 chondrite

Murchison, which have previously been analyzed for Os (Reisberg et al., 2009), Mo (Burkhardt et al., 2012a) and W (Burkhardt et al., 2012b), as well as Sr and Ti isotope anomalies (Burkhardt et al., 2019). Details of this leaching procedure are given in Reisberg et al. (2009) and are briefly summarized in the supplementary information (S1).

2.2. Analytical methods

Zirconium was purified from new digestions and from high-field-strength element (HFSE)-cuts obtained from previous studies using established methods (Render and Brennecka, 2021; Burkhardt et al., 2021). In brief, the Zr-containing cuts were converted into 10 ml 12 M HNO_3 for a first purification employing TODGA resin cartridges as outlined in Torrano et al. (2019). After loading, matrix elements were eluted with an additional 15 ml 12 M HNO_3 . Next, Ti and Fe were eluted with 10 ml 6 M HNO_3 and 10 ml 3 M HNO_3 before Zr was eluted together with Hf in 20 ml 3 M HNO_3 – 0.3 M HF. Following evaporation to dryness, samples were treated with concentrated HNO_3 , dried, and redissolved in 3 M HNO_3 – 1 wt% H_2O_2 to be loaded onto PFA shrink columns containing LN spec resin (100 – 150 mesh) for further separation of Zr from residual Fe, Ti, and Hf (Bast et al., 2015). Finally, solutions were dried, treated with concentrated HNO_3 , dried again, and redissolved in 0.5 M HNO_3 – 0.01 M HF for measurement.

The separation procedure resulted in refined Zr cuts with $\text{Mo}/\text{Zr} < 1 \times 10^{-4}$, $\text{Ru}/\text{Zr} < 1 \times 10^{-4}$, $\text{Ti}/\text{Zr} < 0.1$, $\text{Fe}/\text{Zr} < 0.01$, $\text{Hf}/\text{Zr} < 0.02$, and doping tests were conducted to confirm that these levels were substantially below those that can be accurately corrected. Predilutions of all samples were checked, and any samples exceeding acceptable levels for any element were processed through the second column again. Yields of the entire separation procedure were consistently $>70\%$, and two procedural blanks processed through the same chemical purification procedure contained 150 pg and 340 pg of Zr, which is negligible given that ~ 150 ng of Zr are consumed per analysis.

Measurements were performed on a Neptune Plus MC-ICPMS in Münster and at Lawrence Livermore National Laboratory (LLNL) in combination with a Cetac Aridus II desolvating introduction system using a Jet sampler and H skimmer cone setup, as well as a Savillex C-Flow nebulizer with an uptake rate of 50 $\mu\text{L}/\text{min}$. This setup resulted in intensities for ^{90}Zr between 30 to 40 V for measurement solutions of ~ 200 ng/g (corresponding to a total ion beam intensity of 5.5 to 8×10^{-10} A), while oxide formation rates were adjusted to below 1.5% CeO/Ce. Each measurement consisted of a 30 s baseline and 200 cycles of 4.2 s integration time with all Zr masses (90, 91, 92, 94, and 96) being monitored using 10^{11} Ω amplifiers, while isobaric interferences from Mo and Ru were monitored using 10^{12} Ω amplifiers on masses 95 and 99, respectively. In addition, mass 89 was monitored for potential interferences from doubly-charged Hf ions that correspond to Zr isotope masses; however, measured signals were always $< 1 \times 10^{-3}$ V and appeared more likely to be related to yttrium instead of $^{178}\text{Hf}^{++}$ (the Faraday lineup of the Neptune Plus does not allow mass 89.5 to be set up as part of a Zr cup configuration). Since our doping tests showed that Hf/Zr ratios up to 0.2 do not affect Zr isotope measurement accuracy and all samples had Hf/Zr < 0.02 , we did not apply any corrections related to Hf/Zr. Zirconium isotope data were corrected for mass-bias by internal normalization to $^{94}\text{Zr}/^{90}\text{Zr} = 0.3381$ using the exponential law. Here and throughout the manuscript we employ the μ -notation, denoting parts per million deviations relative to terrestrial standard solutions. In the case of Zr, we use NIST SRM3169 as the

Table 1
Zr isotopic compositions of samples investigated in this study.

Sample	Type	N ^a	$\mu^{91}\text{Zr}^b$	$\mu^{92}\text{Zr}^b$	$\mu^{96}\text{Zr}^b$
BHVO-2 ^c	Basalt	18	1 ± 2	0 ± 2	1 ± 7
BCR-2 ^c	Basalt	17	-1 ± 2	-1 ± 2	-4 ± 4
AGV-2	Andesite	52 (n=2)	0 ± 1	1 ± 1	2 ± 3
Terrestrial average		87	0 ± 1	0 ± 1	1 ± 2
External reproducibility			± 6	± 6	± 18
Zagami ^d	Shergottite	17	-1 ± 2	-1 ± 2	24 ± 4
ALH77005 ^d	Shergottite	10	1 ± 1	-2 ± 2	29 ± 6
EET79001 ^d	Shergottite	9	1 ± 3	0 ± 1	27 ± 9
NWA 8159 ^d	Augite Basalt	8	-2 ± 4	-4 ± 2	29 ± 5
Tissint ^d	Shergottite	8	-2 ± 3	-4 ± 2	25 ± 4
ALH84001 ^d	Orthopyroxenite	13	0 ± 2	-1 ± 2	31 ± 5
Mars average		65 (n=6)	0 ± 1	-2 ± 2	28 ± 3
<i>Non-carbonaceous meteorites</i>					
EET 87746	EH4	5	-1 ± 5	1 ± 0	8 ± 12
Abee	EH4	6	0 ± 3	-1 ± 4	18 ± 7
EH average		11	0 ± 2	0 ± 2	14 ± 6
Atlanta	EL6	8	1 ± 3	-2 ± 2	7 ± 9
ALHA 81021	EL6	4	-5 ± 3	-2 ± 4	10 ± 13
LAP 10014.22	EL6	3	-6 ± 6	-1 ± 6	23 ± 18
Pillistfer	EL6	9	-3 ± 1	-7 ± 1	24 ± 4
Khairpur	EL6	8	-4 ± 3	-3 ± 3	11 ± 7
EL average		32 (n=5)	-3 ± 3	-3 ± 3	15 ± 10
EC average		43 (n=7)	-2 ± 2	-2 ± 2	15 ± 7
Plainview ^c	H5	11	0 ± 2	0 ± 2	34 ± 4
NWA 6299 ^c	H5	10	1 ± 3	0 ± 1	30 ± 6
Nuevo Mercurio	H5	11	1 ± 2	3 ± 2	41 ± 5
H average		32	1 ± 1	1 ± 1	35 ± 3
Tennasilm ^c	L4	10	-1 ± 3	0 ± 2	23 ± 5
Ausson	L5	7	-2 ± 2	0 ± 2	35 ± 5
L average		17	-1 ± 2	0 ± 1	28 ± 5
NWA 5755	LL6	10	4 ± 3	2 ± 2	25 ± 5
NWA 6935	LL5	6	-1 ± 2	-1 ± 2	34 ± 10
St Severin	LL6	7	-3 ± 5	0 ± 3	30 ± 9
Tuxtuac	LL5	6	-2 ± 5	1 ± 4	34 ± 7
LL average		29 (n=4)	0 ± 5	1 ± 2	31 ± 7
OC average		78 (n=9)	0 ± 2	1 ± 1	32 ± 4
LEW 87232	K	5	-1 ± 4	-8 ± 2	42 ± 7
NWA 053	R4	5	1 ± 3	-1 ± 1	23 ± 7
NWA 753	R3.9	5	0 ± 4	-1 ± 3	27 ± 11
NWA 6145	R5	5	-2 ± 4	-1 ± 5	26 ± 4
Rumuruti average		15	0 ± 2	-1 ± 1	25 ± 3
HaH193	Winonaite	4	2 ± 5	0 ± 7	2 ± 9
Fukang	Pallasite	3	1 ± 6	-9 ± 6	43 ± 18
Bishopville	Aubrite	6	-1 ± 4	-7 ± 3	20 ± 6
Pena Blanca Spring	Aubrite	10	-3 ± 2	-8 ± 3	22 ± 6
Aubrite average		16	-2 ± 2	-8 ± 2	21 ± 4
Acapulco	Acapulcoite	7	-1 ± 4	-7 ± 2	35 ± 8
Dho 125	Acapulcoite	6	0 ± 3	-3 ± 2	31 ± 5
Acapulcoite average		13	-1 ± 3	-5 ± 2	33 ± 5
Acfer 063	Mesosiderite	4	1 ± 6	-1 ± 5	32 ± 8
Ilafegh 002	Mesosiderite	5	-1 ± 4	-4 ± 7	41 ± 14
NWA 2538	Mesosiderite	4	-2 ± 7	-2 ± 3	33 ± 17
Mesosiderite average		13	-1 ± 2	-3 ± 2	36 ± 6
Bunburra Rockhole ^c	Achondrite-ung.	5	-4 ± 4	-1 ± 5	13 ± 4
Juvinas ^c	Eucrite	6	1 ± 1	-4 ± 2	18 ± 9
Petersburg ^c	Eucrite	7	0 ± 3	-3 ± 3	28 ± 11
Bouvante ^c	Eucrite	7	-1 ± 3	-4 ± 3	38 ± 10
Millbillillie ^c	Eucrite	6	-4 ± 2	-1 ± 3	45 ± 10
Stannern ^c	Eucrite	6	-4 ± 2	-3 ± 2	44 ± 5
Eucrite average		32 (n=5)	-2 ± 3	-3 ± 1	34 ± 15
NWA 4590 ^c	Angrite	7	3 ± 2	-5 ± 2	54 ± 5
NWA 4801 ^c	Angrite	5	-3 ± 5	-10 ± 2	62 ± 7
NWA 6291 ^c	Angrite	5	0 ± 3	-6 ± 3	46 ± 7
Angra dos Reis ^c	Angrite	6	-1 ± 3	-7 ± 3	45 ± 6
D'Orbigny ^c	Angrite	6	-2 ± 4	-5 ± 2	45 ± 6
NWA 4931	Angrite	9	-1 ± 2	-8 ± 1	47 ± 6
Angrite average		38 (n=6)	-1 ± 2	-7 ± 2	50 ± 7

(continued on next page)

Table 1 (continued)

Sample	Type	N ^a	$\mu^{91}\text{Zr}^{\text{b}}$	$\mu^{92}\text{Zr}^{\text{b}}$	$\mu^{96}\text{Zr}^{\text{b}}$
<i>Carbonaceous meteorites</i>					
Orgueil	CI	1	2 ± 6	7 ± 6	89 ± 18
NWA 13400	CL	7	-4 ± 4	-3 ± 2	103 ± 7
Murchison	CM	7 (n=2)	4 ± 4	3 ± 2	134 ± 6
Allende ('MS-A')	CV3	9 (n=2)	-2 ± 3	-2 ± 2	126 ± 8
DaG 275	CK4/5	7	-1 ± 3	-2 ± 4	123 ± 10
NWA 6604	CK4	5	-2 ± 3	0 ± 1	114 ± 6
CK average		12	-1 ± 2	-1 ± 2	120 ± 6
Kainsaz	CO	7	-1 ± 2	-1 ± 4	114 ± 8
GRA 97755	CR	7	-4 ± 3	-3 ± 3	118 ± 9
Acfer 182	CH3	5	0 ± 2	-2 ± 2	111 ± 9
HaH 237	CBb	2	2 ± 6	1 ± 6	121 ± 18
NWA 6926	Achondrite-ung.	6	-3 ± 0	3 ± 1	124 ± 11
NWA 8548	Achondrite-prim.	7	0 ± 1	3 ± 2	127 ± 4
<i>Murchison leachates</i>					
L1	CM2 leachate	2	296 ± 6	124 ± 6	4998 ± 18
L2	CM2 leachate	1	109 ± 6	46 ± 6	1889 ± 18
L3	CM2 leachate	1	29 ± 6	16 ± 6	507 ± 18
L4	CM2 leachate	1	-66 ± 6	-26 ± 6	-1031 ± 18
L5	CM2 leachate	1	-82 ± 6	-32 ± 6	-1285 ± 18
L6	CM2 leachate	2	-136 ± 6	-56 ± 6	-2064 ± 18

^a Number of overall measurements of a given sample or population, where *n* represents the number of digestions of a given sample or meteorite group.

^b Zr isotope data are expressed in the μ -notation (parts-per-million deviation from the NIST SRM 3169 standard) and internally normalized to $^{94}\text{Zr}/^{90}\text{Zr} = 0.3381$ using the exponential law. Uncertainties are given as Student's *t*-values 95% confidence intervals (95% c.i.) for samples analyzed >3 times or as the external reproducibility as defined by 52 analyses of two digestions of the AGV-2 rock standard (Table S1 in the supplementary information) for samples analyzed ≤3 times. Mean isotopic compositions and associated uncertainties (95% c.i.) for meteorite groups and classes were calculated as averages combining analyses of all meteorite samples assigned to each group and assuming they represent a single population. For meteorite groups with more than 3 separate digestions (EL, EC, LL, OC, Mars, eucrites, and angrites), mean isotopic compositions and related uncertainties (95% c.i.) were calculated from isotopic compositions of the separate digestions.

^c Includes Zr isotope data from Render and Brennecka (2021).

^d Includes Zr isotope data from Burkhardt et al. (2021).

bracketing solution standard, resulting in the example formula below:

$$\mu^i\text{Zr} = \left[\left(\frac{i\text{Zr}}{^{90}\text{Zr}} \right)_{\text{sample}} / \left(\frac{i\text{Zr}}{^{90}\text{Zr}} \right)_{\text{SRM3169}} - 1 \right] \times 10^6$$

The external reproducibility (2 × standard deviation, 2SD) of our methods, as determined by 52 measurements from two digestions of the USGS rock standard AGV-2 processed alongside the samples is ±6 $\mu^{91}\text{Zr}$, ±6 $\mu^{92}\text{Zr}$, and ±18 $\mu^{96}\text{Zr}$ (Table S1). Individual meteorite samples were typically measured between 5-10 times, and results are reported as mean values of pooled solution replicates with their associated 95% confidence intervals.

3. Results

Zirconium isotopic compositions of rock standards and meteorite samples relative to NIST SRM3169 are shown in Table 1 and Figs. 1 and 2. The isotopic compositions of the terrestrial rock standards AGV-2 (andesite from Oregon, USA), BHVO-2 (ocean island basalt from, Hawaii, USA), and BCR-2 (continental basalt from Oregon, USA) are indistinguishable from one another and from the SRM3169 bracketing standard (Table 1). This demonstrates the accuracy of our methods and implies that the Zr isotopic composition of the NIST SRM3169 standard is indistinguishable from bulk Earth. Similarly, a companion study has shown that martian meteorites are isotopically indistinguishable in Zr isotopes, allowing for calculation of a mean isotopic signature for Mars (Burkhardt et al., 2021).

Meteorite samples analyzed in this and the two aforementioned companion studies (Burkhardt et al., 2021; Render and Brennecka, 2021) generally exhibit $\mu^{91}\text{Zr}$ and $\mu^{92}\text{Zr}$ that are indistinguishable or very close (<5 ppm in most instances) to terrestrial Zr isotopic values, with only LEW 87232 (Kakangari chondrite, KC), aubrites, and angrites displaying hints of small deficits

(<10 ppm) in $\mu^{92}\text{Zr}$ (Fig. 2B). Such $\mu^{92}\text{Zr}$ heterogeneity could potentially be radiogenic in origin (Haba et al., 2021), complicating any interpretation of these small anomalies in terms of nucleosynthetic heterogeneity. Given that Nb/Zr ratios were not obtained for all samples and that the $\mu^{92}\text{Zr}$ variations are not or are only barely resolved within the external uncertainty achieved in this study, we do not attach significance to these relatively minor effects.

In contrast, isotopic signatures in ^{96}Zr —the most diagnostic Zr isotope—reveal that Solar System materials are isotopically heterogeneous. Apart from a single winonaite sample and three individual enstatite chondrites, all meteorites investigated here show resolved and variable excesses in $\mu^{96}\text{Zr}$ (Table 1, Fig. 1). The average $\mu^{96}\text{Zr}$ values of the NC chondrites are well defined and increase in the order EC < RC < OC < KC. The $\mu^{96}\text{Zr}$ anomalies in the NC achondrites span a range similar to those of NC chondrites and increase in the order aubrites < acapulcoites ≤ mesosiderites ≤ eucrites ≤ MG pallasites ≤ angrites. Both CC chondrites and achondrites exhibit consistently more anomalous $\mu^{96}\text{Zr}$ compared to their NC counterparts, similar to the higher proportions of neutron-rich isotopes in other elements, such as ^{50}Ti and ^{54}Cr (e.g., Trinquier et al., 2009) or *r*-process Mo (Budde et al., 2016).

The leachates of the Murchison meteorite reveal significantly larger isotope variation compared to the bulk meteorites (Table 1). The magnitude of the anomalies of a given leachate decrease in the order $\mu^{96}\text{Zr} > \mu^{91}\text{Zr} > \mu^{92}\text{Zr}$. The isotope anomalies are well correlated (Fig. 3) and consistently decrease from large excesses in the earlier leaching steps (L1 to L3) to depletions in the later leaching steps (L4 to L6). These isotope systematics and the corresponding slopes in Zr isotope space (Fig. 3) are in excellent agreement with previous sequential acid leachate investigations of other carbonaceous chondrites (Schönbächler et al., 2005; Elfers et al., 2020).

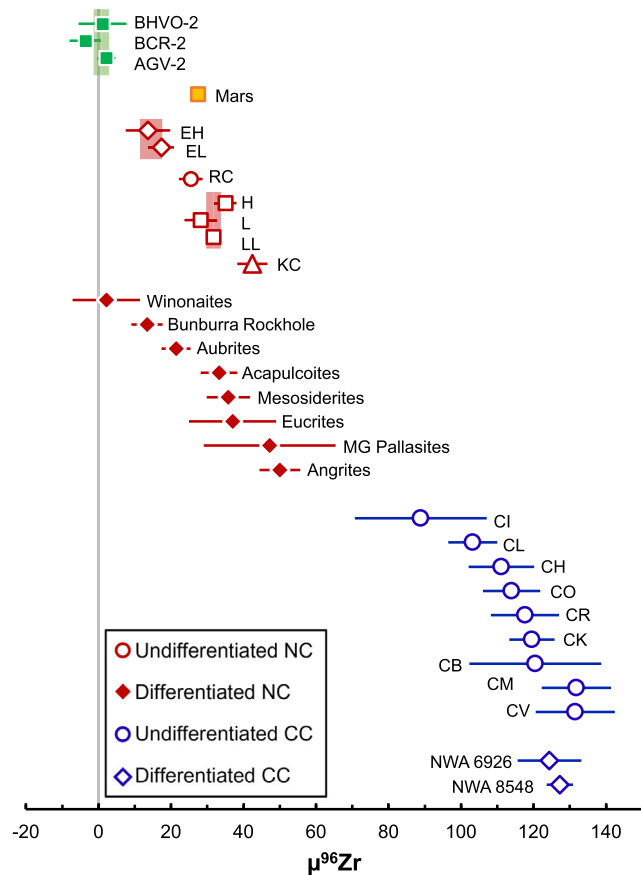


Fig. 1. The $\mu^{96}\text{Zr}$ signatures of terrestrial and meteoritic samples investigated in this study. Isotope data for Mars from Burkhardt et al. (2021) and for Eucrites and Angrites partially from Render and Brennecka (2021). Shaded areas indicate mean compositions for meteorite populations with 95% confidence interval uncertainties. Uncertainties are smaller than the symbols when not visible.

4. Discussion

4.1. Comparison to previous studies

The Zr isotope data set presented in this study is the most comprehensive to date, including the first Zr isotope data for aubrites, acapulcoites, MG pallasites, and winonaites, as well as CL, CH, Rumuruti, and Kakangari chondrites. Furthermore, these data are

more precise compared to most previous data, making it possible to resolve isotope anomalies for most NC meteorites relative to the terrestrial standard and one another. Our data are in overall good agreement with previously published Zr isotope data for several bulk meteorites, but there are also some notable differences, namely with regards to the $\mu^{96}\text{Zr}$ anomalies in carbonaceous chondrites and the extent of $\mu^{91}\text{Zr}$ variations among meteorites. Compared to the results of this study, the $\mu^{96}\text{Zr}$ anomalies of carbonaceous chondrites reported by Akram et al. (2015) tend to be smaller and partly overlap with the compositions of NC meteorites (Fig. 2 and Fig. S1 in the supplementary information). By contrast, all carbonaceous chondrites investigated in this study have well-resolved $\mu^{96}\text{Zr}$ excesses of between ~ 90 and ~ 130 ppm. The cause of the disparate results is unclear at present but may be related to the higher precision achieved in this study. Moreover, the heterogeneous distribution of isotopically anomalous components, such as CAIs, could be a significant contributing factor to the observed isotopic heterogeneity between different aliquots of CC meteorites. For instance, the ~ 40 ppm $\mu^{96}\text{Zr}$ variations among the carbonaceous chondrites can be accounted for by the presence of up to ~ 5 wt.-% CAI, consistent with the observed CAI abundance in CV chondrites and the absence of CAIs in CI chondrites (Fig. 4). However, given the paucity of CAIs in CI chondrites, the heterogeneous distribution of CAIs alone cannot account for the ~ 70 ppm difference between the $\mu^{96}\text{Zr}$ values for Orgueil determined by Akram et al. (2015) ($\mu^{96}\text{Zr} = 24 \pm 22$) and this study ($\mu^{96}\text{Zr} = 89 \pm 18$). We note, however, that the larger ^{96}Zr anomaly obtained here is in line with the ubiquitous ^{96}Zr excesses observed among carbonaceous chondrites and with the idea that the ^{96}Zr variations among carbonaceous chondrites reflect the heterogeneous distribution of CAIs.

We are also unable to confirm a previously suggested $\mu^{91}\text{Zr}$ - $\mu^{96}\text{Zr}$ correlation for whole-rock meteorites (Akram et al., 2015). These authors observed that bulk meteorites plot along a $\mu^{91}\text{Zr}$ - $\mu^{96}\text{Zr}$ trend different than that of acid leachates from primitive meteorites; on this basis, they argued that multiple isotopically variable sources of s-process matter contributed to the early Solar System. In line with Elfers et al. (2020), we find no evidence for significant ^{91}Zr isotope heterogeneity, as variability in $\mu^{91}\text{Zr}$ of all meteorites investigated here is limited to < 5 ppm, smaller than the external reproducibility of the measurements. This is consistent with the suggestion that the previously reported negative $\mu^{91}\text{Zr}$ anomalies of some bulk samples are analytical artifacts resulting from the use of a non-certified solution standard from Alfa Aesar (Akram and Schönbachler, 2016; Elfers et al., 2020). To this

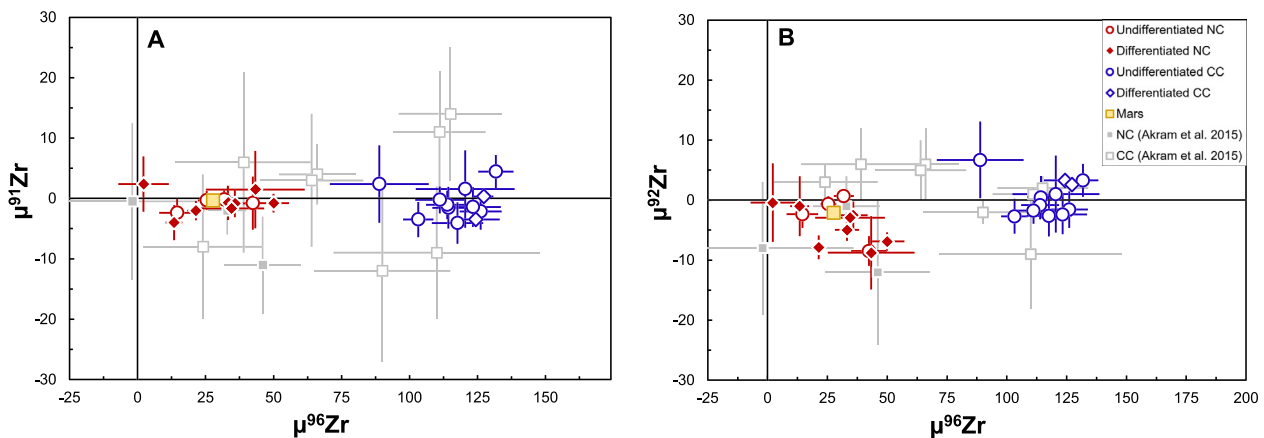


Fig. 2. $\mu^{91}\text{Zr}$ vs. $\mu^{96}\text{Zr}$ and $\mu^{92}\text{Zr}$ vs. $\mu^{96}\text{Zr}$ isotopic compositions of bulk meteorites investigated in this study. Isotope data from Akram et al. (2015) are shown in gray for comparison and have been corrected for a small analytical artifact (Elfers et al., 2020). Whereas the Zr isotope data from Akram et al. (2015) appear to show a continuum of isotopic compositions, new data presented here reveal that the previously reported dichotomy between NC and CC meteorites also exists in Zr isotopes. Uncertainties are smaller than the symbols when not visible.

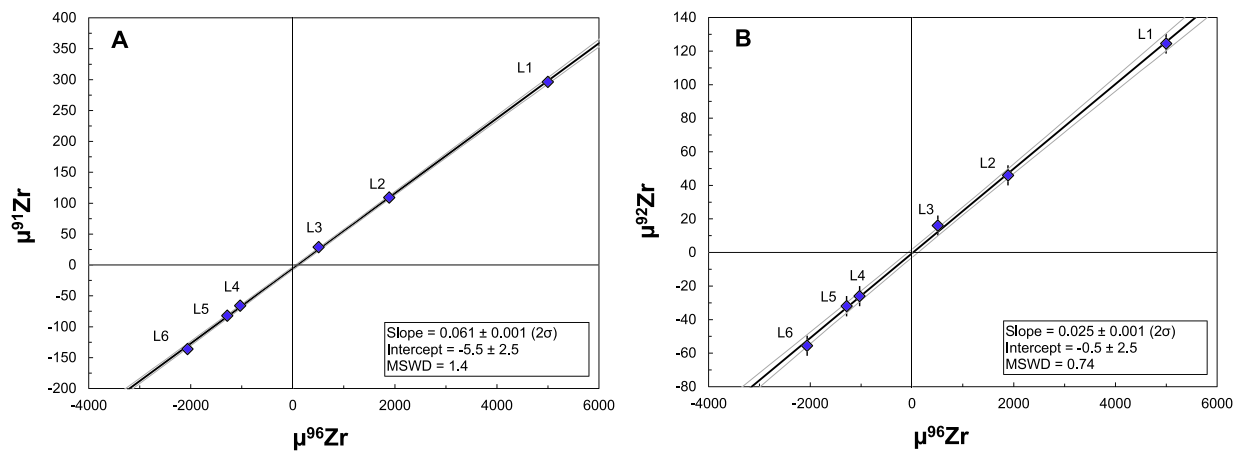


Fig. 3. Plots of (A) $\mu^{91}\text{Zr}$ vs. $\mu^{96}\text{Zr}$ and (B) $\mu^{92}\text{Zr}$ vs. $\mu^{96}\text{Zr}$ of acid leachates of the Murchison carbonaceous chondrite, revealing well-correlated isotope anomalies in all three Zr isotopes. Linear regressions and MSWDs were calculated using Isoplot 4.14. Uncertainties are smaller than the symbols when not visible.

end, we find resolved isotopic differences ($\mu^{91}\text{Zr} = -2.5$, $\mu^{92}\text{Zr} = -2.7$, $\mu^{96}\text{Zr} = 8.2$) between an Alfa Aesar ICP solution and the NIST SRM3169 bracketing standard used here (supplementary information S2), supporting the suggestion that different synthetic solution standards may have distinct Zr isotope compositions.

The lack of resolvable $\mu^{91}\text{Zr}$ variation among bulk meteorites is consistent with the Zr isotope variations in the Murchison acid leachates investigated here: Using the slope and the negative intercept obtained from the linear regression in $\mu^{91}\text{Zr}$ vs. $\mu^{96}\text{Zr}$ of the leachate data (Fig. 3A), we find that for $\mu^{96}\text{Zr} \approx 130$ (i.e., the largest anomaly measured in this study) a $\mu^{91}\text{Zr}$ value of only ~ 2 ppm is expected. This is well within the uncertainty of our Zr isotope measurements and corresponds with the lack of significant $\mu^{91}\text{Zr}$ variation among the samples of this study (Fig. 2A).

4.2. Zr isotope dichotomy between NC and CC meteorites

A key observation from the new Zr isotope data is that NC and CC meteorites have systematically different $\mu^{96}\text{Zr}$ signatures. Unlike in previous work, where NC and CC meteorites showed a continuum of compositions and partly overlapped in $\mu^{96}\text{Zr}$ (Akram et al., 2015), the new data of this study reveal that CC meteorites are characterized by ubiquitous $\mu^{96}\text{Zr}$ excesses of >90 ppm, while NC meteorites all have $\mu^{96}\text{Zr}$ anomalies of <50 ppm (Fig. 1, 2). As such, Zr isotopes conform to the fundamental NC-CC dichotomy observed for several other elements (see summary in Kleine et al., 2020). Analogous to observations for other elements, the new Zr isotope data show that CCs are offset from NCs towards the isotopic composition of CV3 CAIs, corroborating that the CC reservoir is systematically offset from the NC reservoir in the direction of CAIs (Fig. 6, see also Fig. S2 in the supplementary information). On this basis, it has been suggested that the accretion disk initially had a CAI-like isotopic composition (termed ‘IC’ for inclusion-like chondritic reservoir), and late-infalling material with an NC-like isotopic composition caused the observed isotope dichotomy between the inner and outer Solar System by being preferentially added to the inner regions of the protoplanetary disk (Nanne et al., 2019; Burkhardt et al., 2019).

Since in this model the isotopic composition of the CC reservoir results from mixing between two bulk disk reservoirs having distinct isotopic compositions, the fraction of NC material in the CC reservoir should be similar for all elements, irrespective of the geo- and cosmochemical character of these elements. Thus, the new Zr isotope data of this study, and the observation that bulk meteorites display an NC-CC dichotomy for $\mu^{96}\text{Zr}$, can be used to test this pre-

diction. The fraction of NC material in the CC reservoir, f_{NC} , can be calculated by mass balance as follows:

$$f_{\text{NC}} = \frac{\mu_{\text{CC}}^i - \mu_{\text{IC}}^i}{\mu_{\text{NC}}^i - \mu_{\text{IC}}^i}$$

where μ_{CC}^i , μ_{NC}^i , and μ_{IC}^i represent the isotopic anomalies in the CC, NC, and IC reservoirs in a given isotope i . For refractory elements (Ca, Ti, Zr, ...) the isotopic composition of different meteorite groups within the CC reservoir is strongly affected by the admixture of CAIs (Fig. 4). To take this into account, the fraction of NC material in the CC reservoir is most appropriately calculated by substituting μ_{CC}^i with a CAI-free carbonaceous chondrite isotopic composition, which—given their paucity in CAIs—is best represented by CI chondrites (i.e., μ_{CI}^i). For the isotopic composition of the NC reservoir (i.e., μ_{NC}^i) we chose the average isotopic composition of NC meteorites for a given element with the uncertainty covering the entire isotopic range of the NC reservoir. However, the particular choice of μ_{NC}^i in these calculations has little effect on the calculated f_{NC} values; for instance, using the isotopic composition of ureilites, which have the most pronounced anomalies among NC meteorites, for μ_{NC}^i leads to essentially the same results (Table S4). Lastly, the IC (‘Inclusion-like Chondritic’) reservoir is defined by the average isotopic composition of CV3 CAIs (see Table S4 for a summary of all isotope values used in the calculations).

As displayed on Fig. 5, the fraction of NC material in the CC reservoir calculated in this manner for several elements is generally between ~ 0.5 and ~ 0.7 , suggesting that the CC reservoir contains $65 \pm 11\%$ (95% conf.) NC material. This average includes lithophile (Ti, Zr) and siderophile (Mo, Ni) as well as refractory (Ti, Ca, Zr) and main-group elements (Cr, Ni). Similarly, the elements involved are of different nucleosynthetic origins, such as the Fe-group (Ca, Ti, Cr, Ni) and heavier elements (Zr, Mo, Ru). The approximately constant fraction of NC material in the CC reservoir for such a diverse range of elements indicates that the NC-CC dichotomy is unlikely to result from thermal processing of specific presolar carrier phases or the heterogeneous distribution of isotopically anomalous and chemically fractionated components such as CAIs. Instead, to a first order, this constant value is readily accounted for by mixing between two disk reservoirs with similar bulk chemical but distinct isotopic compositions. This observation reinforces earlier proposals that the NC-CC dichotomy results from a combination of disk-wide mixing (with cessation from Jupiter’s formation or another drift barrier in the disk), accompanied by time-varied infall from an isotopically heterogeneous molecular

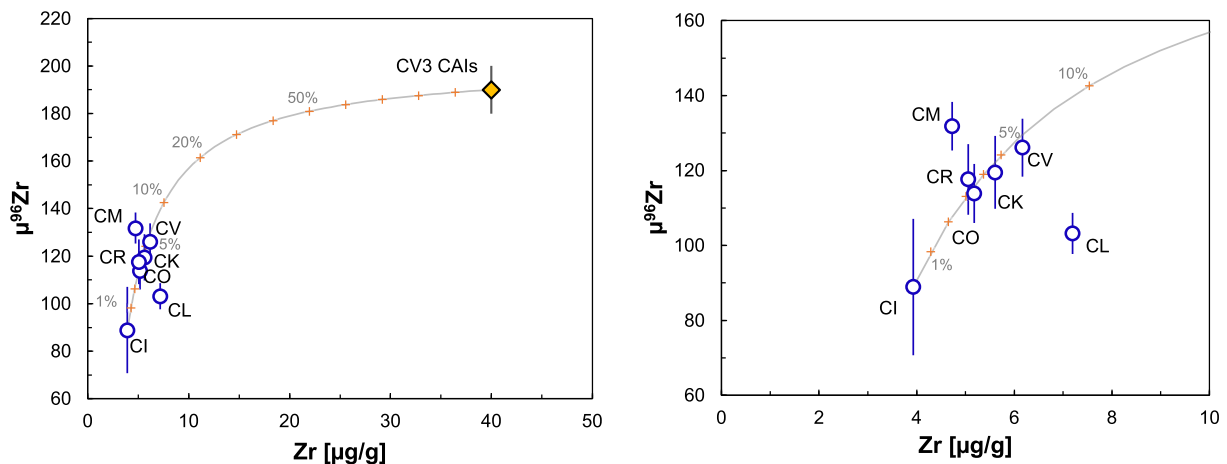


Fig. 4. $\mu^{96}\text{Zr}$ vs. Zr concentration for bulk carbonaceous chondrites. Solid line is a mixing line between CI chondrites and average CV3 CAIs. CM chondrites appear to plot above this mixing trajectory, possibly a result of incorporation of hibonite-rich CAIs in these meteorites (Kööp et al., 2016), whereas CL chondrites plot below the trend, consistent with the interpretation that CL chondrites contain a refractory component that is not characterized by large isotope anomalies (Metzler et al., 2021). Values and references for Zr concentrations and Zr isotope data for CAIs and CCs are summarized in Table S3 in the supplementary information.

cloud core (Nanne et al., 2019; Burkhardt et al., 2019; Jacquet et al., 2019).

Although isotopic anomalies among meteorites and CAIs have been reported for $\mu^{54}\text{Fe}$ (e.g., Shollenberger et al., 2019; Schiller et al., 2020) and $\mu^{84}\text{Sr}$ (e.g., Moynier et al., 2012; Fukai and Yokoyama, 2019; Charlier et al., 2021), our model currently does not include Fe and Sr isotope data. This is because the $\mu^{54}\text{Fe}$ values of CC meteorites ($\mu^{54}\text{Fe}$ range from $\sim +20$ to $\sim +40$, excluding CI chondrites; Hopp et al., 2022) overlap with the average Fe isotopic composition of CAIs ($\mu^{54}\text{Fe} = 43 \pm 17$, Shollenberger et al., 2019), and so calculating the fraction of NC material in the CC reservoir based on Fe isotopes is inconclusive. The lack of clearly resolved Fe isotope anomalies in CAI compared to their host chondrites likely reflects secondary alteration on the meteorite parent bodies, meaning that the original $\mu^{54}\text{Fe}$ of the CAIs were likely larger (Hopp et al., 2022). For Sr, the fraction of NC material in the CC reservoir cannot be calculated because presently available data do not show resolved $\mu^{84}\text{Sr}$ differences between NC and CC meteorites (Fukai and Yokoyama, 2019).

In summary, isotope anomalies for elements of different geo- and cosmochemical character and distinct nucleosynthetic origin consistently show that the characteristic isotopic composition of the CC reservoir can be reproduced by admixture of $\sim 65\%$ NC material to a pre-existing disk having a CAI-like isotopic composition (the IC reservoir). For a refractory element like Zr, additional

isotopic variations among CC chondrites may result from variable abundances of CAI. Interestingly, the two ungrouped carbonaceous achondrites investigated here show similar $\mu^{96}\text{Zr}$ signatures compared to CAI-bearing carbonaceous chondrites. As differentiated meteorites, they likely derive from parent bodies that accreted prior to the carbonaceous chondrite parent bodies. Thus, their elevated $\mu^{96}\text{Zr}$ either point to an early local enrichment of CAI or indicate that these achondrite parent bodies accreted in a region of the CC reservoir with a higher fraction of IC material.

4.3. Isotope heterogeneity within the NC suite of meteorites

Combining the new Zr isotope data with isotopic signatures of other elements reveals significant isotope heterogeneity within meteorites of the NC group, forming well-defined linear correlations of nucleosynthetic anomalies (red solid lines in Fig. 6). These general features of the NC correlations have been described previously (Spitzer et al., 2020; Burkhardt et al., 2021), but so far, the correlations involving Zr were poorly defined, or not defined at all. For instance, the $\mu^{54}\text{Cr}$ vs. $\mu^{96}\text{Zr}$ and $\mu^{94}\text{Mo}$ vs. $\mu^{96}\text{Zr}$ regressions for NC meteorites in Burkhardt et al. (2021) returned R^2 values of 0.47 and 0.65, respectively, and no regression was possible for $\mu^{62}\text{Ni}$ vs. $\mu^{96}\text{Zr}$. With our new Zr isotope data, the R^2 values for $\mu^{54}\text{Cr}$ vs. $\mu^{96}\text{Zr}$ and $\mu^{94}\text{Mo}$ vs. $\mu^{96}\text{Zr}$ are improved to 0.83 and 0.80, respectively, and our $\mu^{64}\text{Ni}$ vs. $\mu^{96}\text{Zr}$ regression yields an R^2 of 0.86.

Importantly, the isotopes used in Fig. 6 ($\mu^{48}\text{Ca}$, $\mu^{50}\text{Ti}$, $\mu^{54}\text{Cr}$, $\mu^{64}\text{Ni}$, $\mu^{94}\text{Mo}$, $\mu^{96}\text{Zr}$, and $\mu^{100}\text{Ru}$) belong to elements with variable condensation temperatures, and include lithophile (Ca, Ti, Cr, Zr) and siderophile (Ni, Mo, Ru) as well as Fe-peak (Ca, Ti, Cr, Ni) and higher-mass elements (Zr, Mo, Ru), making it highly unlikely for these elements to be hosted in roughly similar proportions in the same presolar carrier phases or dust components. Thus, the selective removal (or addition) of a single presolar phase—for instance, by thermal processing in the inner disk—and selective dust-sorting are unlikely explanations for the isotope heterogeneity in the NC region, as they would not be expected to result in the observed linear trends in multi-element isotope space. As such, although individual presolar grains such as mainstream SiC are an attractive candidate phase that could be responsible for some of the observed isotope variations (e.g., in Zr), the heterogeneous distribution of such components is unlikely to be the main driver of isotope variations among NC meteorites. Instead, the linear correlations in elements of variable geo- and cosmochemical nature or

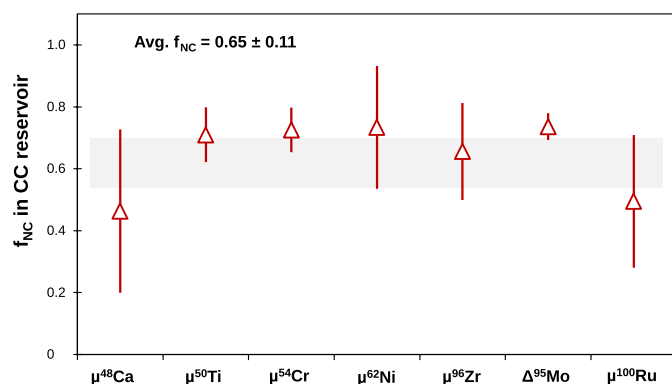


Fig. 5. Fraction of NC material in the CC reservoir calculated by mass balance (see section 4.2) for several elements, including Zr from this study. An average of these seven elements suggests the CC reservoir to consist of roughly two thirds NC material. Isotopic compositions used for these calculations are given in Table S4 in the supplementary information.

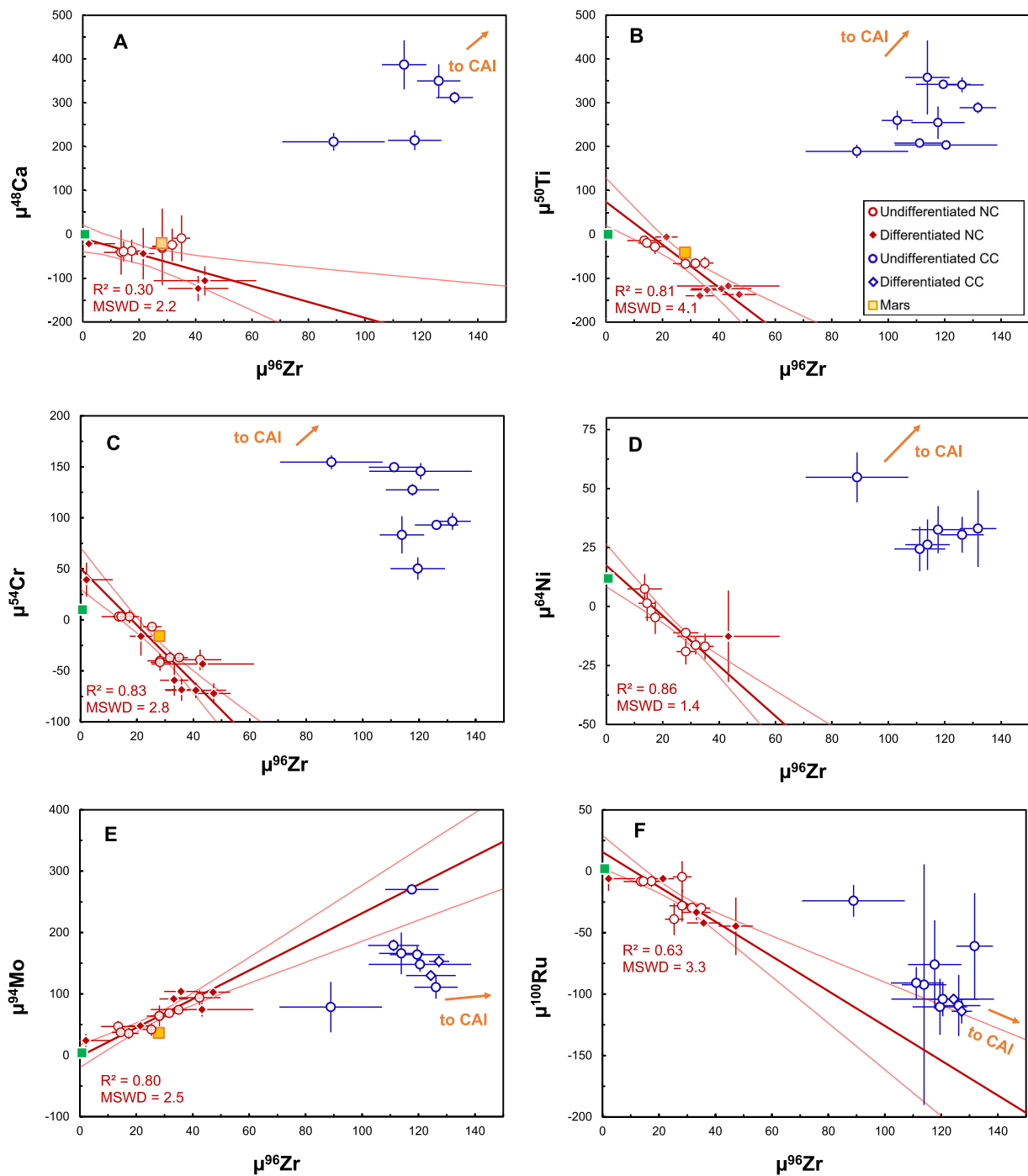


Fig. 6. Multi-element nucleosynthetic isotope variations in bulk meteorites and terrestrial planets. Nucleosynthetic isotope anomalies in $\mu^{96}\text{Zr}$ are correlated with those of other elements within the suite of non-carbonaceous meteorites, however, these trends do not systematically point toward the CC reservoir or CAIs [the anomalous Mo isotopic composition for Murchison from Burkhardt et al. (2011) was excluded from panel E]. A version of this figure including mixing trajectories between the NC and CAI isotopic compositions can be found in the supplementary information (Figure S2). Concentration and isotope data for Ca, Ti, Cr, Ni, Mo, and Ru were taken from Burkhardt et al. (2019) and Spitzer et al. (2020). Linear regressions were calculated using Isoplot 4.14.

stellar origin are most easily accounted for by mixing two chemically similar—but isotopically different—components.

Although both the NC-CC dichotomy as well as the isotope variations within the NC reservoir were likely generated by mixing between isotopically distinct bulk disk reservoirs, the mixing components involved must have been different. This is because the NC regressions shown in Fig. 6 point toward the CAI-like isotopic composition only in Zr, Mo, and Ru isotope space (panels E, F), whereas for plots of Fe-group elements vs. Zr (or Mo, Ru), the NC trends are almost perpendicular to the NC-CAI offset (panels A-D). This sug-

gests that the origin of isotope heterogeneity among NC meteorites cannot be related to the admixture of CAIs or CAI-like matter, as is the case for carbonaceous chondrites, but must have a distinct or additional cause. Nevertheless, when only the Fe-group elements are considered, the NC trend points toward the composition measured for CAIs, suggesting that the NC trend may have been produced by the same mixing processes that also established the NC-CC dichotomy. These seemingly contradictory observations can be reconciled if one endmember producing the NC trend had CAI-like excesses in the neutron-rich isotopes of Fe-peak elements (i.e.,

high $\mu^{48}\text{Ca}$, $\mu^{50}\text{Ti}$, $\mu^{54}\text{Cr}$, $\mu^{62}\text{Ni}$) but was enriched in *s*-process nuclides (i.e., low $\mu^{96}\text{Zr}$ and $\mu^{94}\text{Mo}$ and high $\mu^{100}\text{Ru}$), unlike most measured CAIs. This putative component has been termed ‘s-IC’ for *s*-enriched inclusion-like component (Spitzer et al., 2020); however, the origin of this component and how it relates to CAIs and the early disk reservoir having a CAI-like isotopic composition remains elusive. More work is needed to assess whether evidence for such an *s*-process-enriched component exists among the components of primitive chondrites. The results of this study show that Zr isotope measurements are a promising tool to search for this material, as Zr is abundant in various chondrite components and can readily be used to identify *s*-process enriched matter.

4.4. Spatial vs. temporal isotope heterogeneity in the early Solar System

The isotopic variations among NC meteorites could be either temporal or spatial in nature, or a combination thereof. For example, Schiller et al. (2018) and Frossard et al. (2021) argue for a temporal evolution in the isotopic composition of the protoplanetary disk during planetesimal accretion, based on Ca and Nd isotopes, respectively. Other studies have instead highlighted relationships between nucleosynthetic isotope anomalies in several elements (including Mo, Ru, and Nd) and heliocentric formation distance (e.g., Trinquier et al., 2007; Yamakawa et al., 2010; Burkhardt et al., 2011; Fischer-Gödde and Kleine, 2017; Render and Brenneka, 2021). Zirconium isotopes represent a powerful tool to potentially distinguish between these two options, as nucleosynthetic anomalies of lithophile elements in the silicate mantles of planetary materials are unlikely to have been overprinted by late-stage impacts, as could be the case for the siderophile elements Mo and Ru. To distinguish between a temporal and spatial isotopic heterogeneity, we first review available parent body accretion ages for NC meteorites analyzed for Zr isotopes in this study, and then assess whether systematic isotopic differences exist between samples from early- and late-formed parent bodies, which would be expected if the NC trend reflects temporal variations.

The parent bodies of differentiated meteorites are thought to have formed very early in Solar System history, when the short-lived radionuclide ^{26}Al was still sufficiently abundant to have facilitated partial melting and planetary differentiation (Hevey and Sanders, 2006). This is consistent with parent body accretion ages of <1 Ma after CAI formation determined for differentiated meteorites such as iron meteorites, angrites, and eucrites (see summary in Spitzer et al., 2020 and references therein). For other differentiated meteorites, including the aubrites, mesosiderites, and MG pallasites, parent body accretion ages are less well known. Based on thermal modeling the accretion age of the aubrite parent body has been estimated to be <1.5 Ma after CAI formation (Sugiura and Fujiya, 2014). Mesosiderites and pallasites likely formed by collisional mixing of metal and silicate from different bodies, and so it is reasonable to assume that the accretion ages of these progenitor bodies were similar to those of other differentiated meteorites, i.e., <1 Ma after CAI formation. Another important group of meteorites are primitive achondrites—such as the acapulcoites/lo-dranites and winonaites—which are thought to derive from parent bodies that underwent only partial differentiation. On the basis of thermochronological data and thermal modeling, the accretion age of the acapulcoite-lo-dranite parent body has been estimated to be 1.7 ± 0.3 Ma after CAI formation (Touboul et al., 2009; Neumann et al., 2019), suggesting that this object formed later than the parent bodies of fully differentiated meteorites. The accretion age of the winonaite parent body is less well known, but based on the undifferentiated nature of winonaites and the only small degree of incipient melting an accretion age of ~ 1.8 Ma after CAI has been estimated, with no uncertainty given on this estimate (Hunt et al., 2017). Finally, accretion ages for NC chondrite parent bodies have

been constrained either through ages of chondrules or the combination of thermochronological data and thermal modeling. For instance, the chondrule ages from the most primitive ordinary chondrites suggest a parent body accretion age of 1.8 ± 0.1 Ma after CAI formation (Pape et al., 2019), consistent with thermochronological data (e.g., Edwards and Blackburn, 2020) and thermal modeling (e.g., Henke et al., 2012). For enstatite chondrites no chondrule ages are available, but thermochronological data suggest an accretion age of 1.95 ± 0.15 Ma after CAI formation (Trieloff et al., 2022). For Rumuruti and Kakangari chondrites no chronological data are available to evaluate parent body accretion ages, but given their undifferentiated nature it is reasonable to assume that they, like the enstatite and ordinary chondrites, formed at about 2 Ma after CAI formation, when the abundance of ^{26}Al was too low to cause melting.

If temporal changes were mainly responsible for isotopic heterogeneity within the suite of NC meteorites, one would expect to see a trend between $\mu^{96}\text{Zr}$ and formation age, with a gradual change in $\mu^{96}\text{Zr}$ values from early-formed differentiated samples, followed by partially differentiated (i.e., primitive) achondrites, and then later-formed chondritic samples. However, in contrast to these expectations, we here find that differentiated meteorites like aubrites and angrites collectively span a range from 15 to 50 in $\mu^{96}\text{Zr}$, which is indistinguishable from that occupied by enstatite, ordinary, Rumuruti, and Kakangari chondrites that formed later in Solar System history (Fig. 7). Winonaites and acapulcoites-lo-dranites, which both derive from parent bodies that accreted later than those of the fully differentiated achondrites but probably slightly earlier than the chondrite parent bodies, also exhibit a similar range in $\mu^{96}\text{Zr}$ from 2 to 33 (Fig. 7). Hence, it seems unlikely that temporal changes (alone) are responsible for the isotope heterogeneity observed among NC meteorites. Instead, the data presented in this work support the interpretation that the heterogeneous distribution of isotopically anomalous matter in the protoplanetary disk primarily occurred on a spatial level. Nevertheless, isotopic variations among the early-formed parent bodies of differentiated NC meteorites may still reflect temporal changes related to a rapidly changing composition of the disk during infall (Spitzer et al., 2020; Morbidelli et al., 2022). This hypothesis is difficult to test, however, because the inferred parent body accretion

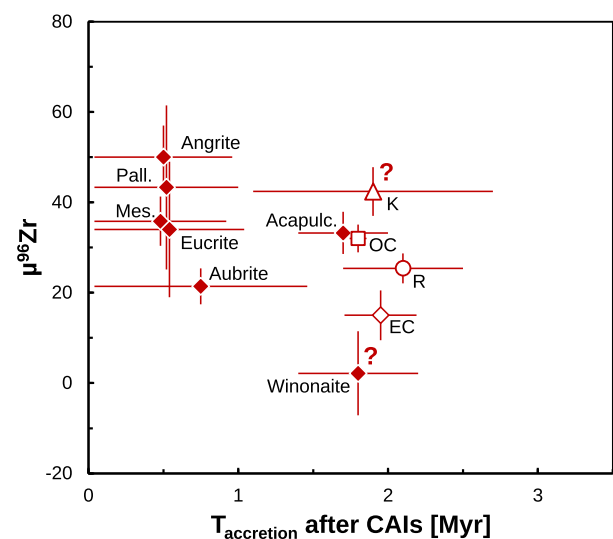


Fig. 7. $\mu^{96}\text{Zr}$ isotope signatures plotted against accretion time after Solar System formation, indicating no systematic changes in the isotopic composition of the protoplanetary disk over time. Accretion ages of various Solar System materials are given in the main text. Labels correspond to: Pall.-Main group pallasites; Mes.-Mesosiderites; Acapulc.-Acapulcoites; EC-enstatite chondrites; OC-ordinary chondrites; R-Rumuruti chondrites; K-Kakangari chondrites.

ages of these objects are all <1 Ma after CAI formation and their accretion ages are not resolved from each other.

4.5. The role of meteorite parent bodies in constructing the terrestrial planets

Nucleosynthetic isotope anomalies provide a powerful tool for reconstructing the origin and nature of the terrestrial planets' building materials, which in turn is key for constraining the dynamic processes by which planets formed. In the classic accretion model, the terrestrial planets grow by the collisions among Moon-to-Mars-sized planetary embryos and planetesimals from the inner Solar System, with only little contribution from outer Solar System objects scattered into the inner disk during the growth and migration of the giant planets (e.g., Chambers and Wetherill, 1998; Raymond and Izidoro, 2017). Previous work has shown that this formation model is consistent with the isotopic composition of Earth and Mars, which can be reproduced by a combination of inner Solar System bodies with only minor contribution of CC bodies from the outer Solar System (Dauphas, 2017; Burkhardt et al., 2021). However, an alternative model has been proposed, in which the terrestrial planets grow by accreting large amounts of pebbles from the outer Solar System which drift sunward through the disk because of gas drag (e.g., Ormel and Klahr, 2010). By looking at just a subset of elements, namely Ca and Fe, it has been suggested that this model is consistent with nucleosynthetic isotope signatures (Johansen et al., 2021), because the isotope compositions of these elements may be interpreted to indicate a large fraction of CC material (~40 % by mass) in Earth and Mars (Schiller et al., 2018, 2020). Other work has shown, however, that a large fraction of CC material in Earth and Mars is inconsistent with the isotopic signatures of other Fe-group elements such as Ni and Cr (Hopp et al., 2022). Moreover, by simultaneously considering all elements for which nucleosynthetic isotope heterogeneity exists at the bulk scale, Burkhardt et al. (2021) showed that Earth and Mars incorporated only a small fraction of CC material, which is inconsistent with a pebble accretion origin for these planets.

The disparate conclusions drawn from nucleosynthetic isotope signatures highlight a fundamental problem when using isotope anomalies to reconstruct terrestrial planet formation, namely the issue of whether meteorites are representative of the material that built the planets. Previous work has shown that Earth is enriched in *s*-process matter relative to most meteorites, which is most clearly seen for Mo (Burkhardt et al., 2011; Budde et al., 2019) but also for Nd (Burkhardt et al., 2016) and Ru (Fischer-Gödde and Kleine, 2017). Unlike the siderophile elements Mo and Ru, which record the late stages of terrestrial planet growth (Dauphas, 2017), Zr, as a lithophile element, provides information on the heritage of all the material accreted by Earth over its entire growth history. This makes Zr ideally suited to assess the origin and nature of the bulk building material of the terrestrial planets. As previous Zr isotope studies found no resolvable variations among NC meteorites, or between Earth and enstatite chondrites (Akram et al., 2015), Zr isotopes had been of limited use for characterizing the building material of Earth. However, with our increased precision, we not only find Zr isotope variations among NC meteorites but also show that enstatite chondrites are characterized by *s*-process deficits compared to Earth, in good agreement with isotope studies of other elements (e.g., Burkhardt et al., 2016; Fischer-Gödde and Kleine, 2017; Render et al., 2017). At the current analytical precision, only winonaites appear to exhibit Zr isotopic compositions indistinguishable from the BSE, but given their isotope anomalies in other elements (e.g., Schiller et al., 2015), winonaites are an unsuitable match as the primary potential terrestrial building blocks. Thus, the terrestrial Zr isotope signature demonstrates that the average building material of Earth as a whole, and not only its late-

stage building blocks, was enriched in *s*-process matter compared to meteorites. Considering the previously highlighted relationship between nucleosynthetic isotope anomalies and (presumed) heliocentric distance (Yamakawa et al., 2010; Burkhardt et al., 2011; Fischer-Gödde and Kleine, 2017; Render and Brenneka, 2021), this *s*-process-enriched building material most likely is from the innermost Solar System (Burkhardt et al., 2021).

A corollary of this observation is that meteorites alone cannot be used to identify Earth's building material, even for elements for which the terrestrial isotopic composition lies within the range of meteorite compositions. For instance, it has been suggested that Earth consists of ~40% CC material because the BSE's isotopic composition for the Fe-peak elements (^{48}Ca , ^{50}Ti , ^{54}Cr ...) is intermediate between NC and CC meteorites (Schiller et al., 2018, 2020). However, as demonstrated in Fig. 6, in each of the multi-elemental panels the BSE occupies an endmember isotopic composition on the NC trend, exhibiting not only the most neutron-rich (for Fe-peak elements) but also the most *s*-enriched (for higher-mass elements) composition within the NC reservoir. Consequently, the BSE's isotopic signature for Fe-group elements (i.e., more elevated $\mu^{48}\text{Ca}$, $\mu^{50}\text{Ti}$, $\mu^{54}\text{Cr}$ etc. compared to NC meteorites) does not reflect the addition of CC material from the outer Solar System, but a larger contribution of the *s*-process-enriched building material from the inner Solar System. This example highlights the severe limitations that may result from only considering isotope anomalies for Fe-group elements to identify the nature and origin of Earth's building material.

The overall *s*-process-enriched nature of Earth makes elements exhibiting *s*-process variations particularly important for reconstructing Earth's accretion history. With the new Zr isotope data of this study, there is now a comprehensive data set for three elements (Zr, Mo, Ru), which not only are characterized by *s*-process variations among Solar System materials, but also exhibit distinct geochemical behavior. As such, these three elements record different stages of Earth's accretion, where Zr provides an integrated signature of Earth's entire accretion while Mo records the last 10–20% and Ru the last ~0.5% (i.e., the late veneer) (Dauphas, 2017). Thus, the observation that BSE plots within uncertainty of the NC trends in Mo-Zr and Ru-Zr isotope space indicates that the provenance of Earth's building material has not changed significantly as accretion proceeded. This and the observation that BSE is not offset from the NC trends towards the CC reservoir demonstrates that CC meteorites cannot have contributed significantly to the growth of the terrestrial planets. This is consistent with previous suggestions of only ~4% by mass of CC material in bulk Earth and is also consistent with a similarly low fraction of CC materials inferred of Mars (Burkhardt et al., 2021). Recently published Zn isotope data appear to confirm such limited CC fractions and indicate that outer Solar System contributions likely happened late in Earth's accretion history (Savage et al., 2022; Steller et al., 2022). Collectively, the currently available inventory of isotope data in all elements therefore precludes a pebble accretion scenario for the formation of the terrestrial planets.

5. Conclusions

New Zr isotope data for a broad set of differentiated and undifferentiated meteorites of both NC and CC pedigree reveal that nearly all samples—including enstatite chondrites—exhibit resolvable excesses in ^{96}Zr relative to terrestrial Zr. Meteorites from the CC reservoir are consistently more anomalous compared to NC meteorites, demonstrating that the NC-CC isotope dichotomy previously described for other elements also includes Zr isotopes. Furthermore, meteorites within the NC suite exhibit $\mu^{96}\text{Zr}$ variation that is correlated with isotope anomalies in other elements. Given the differences in nucleosynthetic provenance, as well as

geo- and cosmochemical character of the elements involved, this argues against thermal processing and selective dust-sorting in the disk as the main responsible cause for generating this planetary-scale isotope heterogeneity, both for the formation of the NC-CC dichotomy and the correlated isotope variations among NC meteorites. Instead, this isotope heterogeneity is readily explained as the result of mixing isotopically distinct reservoirs with (near-) solar chemical compositions, where this mixing likely occurred during infall from an isotopically heterogeneous molecular cloud core during the early stages of disk building. Within this framework, the isotopic composition of the CC reservoir can be accounted for by late-stage infall of NC-like material onto a pre-existing disk having a CAI-like isotopic composition, with mass balance calculations suggesting that the fraction of NC material in the CC reservoir is ~ 0.65 , for Zr and all other elements exhibiting the NC-CC dichotomy. The correlated isotope variations among NC meteorites may likewise reflect mixing during infall, but the origin of the mixing endmembers involved is less well understood.

The consistent excesses of $\mu^{96}\text{Zr}$ throughout all studied meteorite groups imply that Earth is overall enriched in *s*-process isotopes compared to known meteorites and that our meteorite collections are lacking a substantial component of the terrestrial building material. Meteorites of CC pedigree appear to have not been involved in the accretion histories of the terrestrial planets to a significant degree, which indicates formation of the terrestrial planets from material of the inner Solar System and argues against formation by pebble accretion.

CRediT authorship contribution statement

Jan Render: Conceptualization, Investigation, Methodology, Writing – original draft. **Gregory A. Brenneka:** Conceptualization, Funding acquisition, Resources, Supervision, Writing – review & editing. **Christoph Burkhardt:** Resources, Writing – review & editing. **Thorsten Kleine:** Funding acquisition, Resources, Supervision, Writing – review & editing.

Declaration of competing interest

The authors declare that they have no known competing financial interests or personal relationships that could have appeared to influence the work reported in this paper.

Data availability

All data generated during this study are included in this article (and its supplementary information files).

Acknowledgements

Reviews by T. Iizuka and an anonymous referee enhanced the manuscript and are greatly appreciated. F. Moynier is thanked for swift editorial handling. The authors furthermore thank Gerit Budde, Jonas Schneider, David Sievert, Elias Wölfer, and Emily Worsham for providing samples. This work was partially funded by a Sofja Kovalevskaja Award from the Alexander von Humboldt Foundation (G.A.B.). C.B. and T.K. were supported by the Deutsche Forschungsgemeinschaft (German Research Foundation)—Project ID 263649064-TRR170. This is TRR pub. no. 165. This study was performed under the auspices of the US DOE by Lawrence Livermore National Laboratory under Contract DE-AC52-07NA27344 with release number LLNL-JRNL-832802.

Appendix A. Supplementary material

Supplementary material related to this article can be found online at <https://doi.org/10.1016/j.epsl.2022.117748>.

References

- Akram, W., Schönbächler, M., Sprung, P., Vogel, N., 2013. Zirconium–hafnium isotope evidence from meteorites for the decoupled synthesis of light and heavy neutron-rich nuclei. *Astrophys. J.* 777, 169–181.
- Akram, W., Schönbächler, M., Bisterzo, S., Gallino, R., 2015. Zirconium isotope evidence for the heterogeneous distribution of *s*-process materials in the solar system. *Geochim. Cosmochim. Acta* 165, 484–500.
- Akram, W., Schönbächler, M., 2016. Zirconium isotope constraints on the composition of Theia and current Moon-forming theories. *Earth Planet. Sci. Lett.* 449, 302–310.
- Bast, R., Scherer, E.E., Sprung, P., Fischer-Gödde, M., Stracke, A., Mezger, K., 2015. A rapid and efficient ion-exchange chromatography for Lu–Hf, Sm–Nd, and Rb–Sr geochronology and the routine isotope analysis of sub-ng amounts of Hf by MC-ICP-MS. *J. Anal. At. Spectrom.* 30, 2323–2333.
- Budde, G., Burkhardt, C., Brenneka, G.A., Fischer-Gödde, M., Kruijjer, T.S., Kleine, T., 2016. Molybdenum isotopic evidence for the origin of chondrules and a distinct genetic heritage of carbonaceous and non-carbonaceous meteorites. *Earth Planet. Sci. Lett.* 454, 293–303.
- Budde, G., Burkhardt, C., Kleine, T., 2019. Molybdenum isotopic evidence for the late accretion of outer solar system material to Earth. *Nat. Astron.* 3, 736–741.
- Burkhardt, C., Kleine, T., Oberli, F., Pack, A., Bourdon, B., Wieler, R., 2011. Molybdenum isotope anomalies in meteorites: constraints on solar nebula evolution and origin of the Earth. *Earth Planet. Sci. Lett.* 312, 390–400.
- Burkhardt, C., Klein, T., Dauphas, N., Wieler, R., 2012a. Origin of isotopic heterogeneity in the solar nebula by thermal processing and mixing of nebular dust. *Earth Planet. Sci. Lett.* 357–358, 298–307.
- Burkhardt, C., Kleine, T., Dauphas, N., Wieler, R., 2012b. Nucleosynthetic tungsten isotope anomalies in acid leachates of the Murchison chondrite: implications for Hf–W chronometry. *Astrophys. J. Lett.* 753, L6.
- Burkhardt, C., Borg, L.E., Brenneka, G.A., Shollenberger, Q.R., Dauphas, N., Kleine, T., 2016. A nucleosynthetic origin for the Earth's anomalous ^{142}Nd composition. *Nature* 537, 394–398.
- Burkhardt, C., Dauphas, N., Hans, U., Bourdon, B., Kleine, T., 2019. Elemental and isotopic variability in solar system materials by mixing and processing of primordial disk reservoirs. *Geochim. Cosmochim. Acta* 261, 145–170.
- Burkhardt, C., Spitzer, F., Morbidelli, A., Budde, G., Render, J., Kruijjer, T.S., Kleine, T., 2021. Terrestrial planet formation from lost inner solar system material. *Sci. Adv.* 7, eabj7601.
- Chambers, J.E., Wetherill, G.W., 1998. Making the terrestrial planets: N-body integrations of planetary embryos in three dimensions. *Icarus* 136, 304–327.
- Charlier, B.L.A., Tissot, F.L.H., Vollstaedt, H., Dauphas, N., Wilson, C.J.N., Marquez, R.T., 2021. Survival of presolar p-nuclide carriers in the nebula revealed by stepwise leaching of Allende refractory inclusions. *Sci. Adv.* 7, eabf6222.
- Dauphas, N., 2017. The isotopic nature of the Earth's accreting material through time. *Nature* 541, 521–524.
- Edwards, G.H., Blackburn, T., 2020. Accretion of a large LL parent planetesimal from a recently formed chondrule population. *Sci. Adv.* 6, eaay8641.
- Ek, M., Hunt, A.C., Lugaro, M., Schönbächler, M., 2020. The origin of *s*-process isotope heterogeneity in the solar protoplanetary disk. *Nat. Astron.* 4, 273–281.
- Elfers, B.-M., Sprung, P., Messling, N., Münker, C., 2020. The combined Zr and Hf isotope inventory of bulk rock and sequentially leached chondrite samples. *Geochim. Cosmochim. Acta* 270, 475–491.
- Fischer-Gödde, M., Kleine, T., 2017. Ruthenium isotopic evidence for an inner solar system origin of the late veneer. *Nature* 541, 525–527.
- Frossard, P., Guo, Z., Spencer, M., Boyet, M., Bouvier, A., 2021. Evidence from achondrites for a temporal change in Nd nucleosynthetic anomalies within the first 1.5 million years of the inner solar system formation. *Earth Planet. Sci. Lett.* 566, 116968.
- Fukai, R., Yokoyama, T., 2019. Nucleosynthetic Sr–Nd isotope correlations in chondrites: evidence for nebular thermal processing and dust transportation in the early solar system. *Astrophys. J.* 879, 79–90.
- Goldmann, A., Brenneka, G.A., Noordmann, J., Weyer, S., Wadhwa, M., 2015. The uranium isotopic composition of the Earth and the solar system. *Geochim. Cosmochim. Acta* 148, 145–158.
- Haba, M.K., Lai, Z.-J., Wotzlaw, J.-F., Yamaguchi, A., Lugaro, M., Schönbächler, M., 2021. Precise initial abundance of Niobium-92 in the solar system and implications for *p*-process nucleosynthesis. *Proc. Natl. Acad. Sci. USA* 118, e2017750118.
- Hevey, P.J., Sanders, I.S., 2006. A model for planetesimal meltdown by ^{26}Al and its implications for meteorite parent bodies. *Meteorit. Planet. Sci.* 41, 95–106.
- Hopp, T., Budde, G., Kleine, T., 2020. Heterogeneous accretion of Earth inferred from Mo–Ru isotope systematics. *Earth Planet. Sci. Lett.* 534, 116065.
- Hopp, T., Dauphas, N., Spitzer, F., Burkhardt, C., Kleine, T., 2022. Earth's accretion inferred from iron isotopic anomalies of supernova nuclear statistical equilibrium origin. *Earth Planet. Sci. Lett.* 577, 117245.
- Hunt, A.C., Benedix, G.K., Hammond, S.J., Bland, P.A., Rehkämper, M., Kreissig, K., Strekopytov, S., 2017. A geochemical study of the winonaites: evidence for limited partial melting and constraints on the precursor composition. *Geochim. Cosmochim. Acta* 199, 13–30.

- lizuka, T., Lai, Y.-J., Akram, W., Amelin, Y., Schönbächler, M., 2016. The initial abundance and distribution of ^{92}Nb in the solar system. *Earth Planet. Sci. Lett.* 439, 172–181.
- Jacquet, E., Pignatale, F.C., Chaussidon, M., Charnoz, S., 2019. Fingerprints of the protosolar cloud collapse in the solar system. II. Nucleosynthetic anomalies in meteorites. *Astrophys. J.* 884, 32–42.
- Johansen, A., Ronnet, T., Bizzarro, M., Schiller, M., Lambrechts, M., Nordlund, A., Lammer, H., 2021. A pebble accretion model for the formation of the terrestrial planets in the solar system. *Sci. Adv.* 7, eabc0444.
- Kleine, T., Budde, G., Burkhardt, C., Kruijjer, T.S., Worsham, E.A., Morbidelli, A., Nimmo, F., 2020. The non-carbonaceous-carbonaceous meteorite dichotomy. *Space Sci. Rev.* 216, 55.
- Kööp, L., Davis, A.M., Nakashima, D., Park, C., Krot, A.N., Nagashima, K., Tenner, T.J., Heck, P.R., Kita, N.T., 2016. A link between oxygen, calcium and titanium isotopes in ^{26}Al -poor hibonite-rich CAIs from Murchison and implications for the heterogeneity of dust reservoirs in the solar nebula. *Geochim. Cosmochim. Acta* 189, 70–95.
- Kruijjer, T.S., Burkhardt, C., Budde, G., Kleine, T., 2017. Age of Jupiter inferred from the distinct genetics and formation times of meteorites. *Proc. Natl. Acad. Sci.* 114, 6712–6716.
- Leya, I., Wieler, R., Halliday, A.N., 2003. The influence of cosmic-ray production on extinct nuclide systems. *Geochim. Cosmochim. Acta* 67, 529–541.
- Metzler, K., Hezel, D.C., Barosch, J., Wölfer, E., Schneider, J.M., Hellmann, J.L., Berndt, J., Stracke, A., Gattacceca, J., Greenwood, R.C., Franchi, I.A., Burkhardt, C., Kleine, T., 2021. The Loongana (CL) group of carbonaceous chondrites. *Geochim. Cosmochim. Acta* 304, 1–31.
- Morbidelli, A., Baillié, K., Batygin, K., Charnoz, S., Guillot, T., Rubie, D.C., Kleine, T., 2022. Contemporary formation of early solar system planetesimals at two distinct radial locations. *Nat. Astron.* 6, 72–79.
- Henke, S., Gail, H.P., Trieloff, M., Schwarz, W.H., Kleine, T., 2012. Thermal evolution and sintering of chondritic planetesimals. *Astron. Astrophys.* 537.
- Moynier, F., Day, J.M.D., Okui, W., Yokoyama, T., Bouvier, A., Walker, R.J., Podosek, F.A., 2012. Planetary-scale strontium isotopic heterogeneity and the age of volatile depletion of early solar system materials. *Astrophys. J.* 758, 45–51.
- Nanne, J.A.M., Nimmo, F., Cuzzi, J.N., Kleine, T., 2019. Origin of the non-carbonaceous-carbonaceous meteorite dichotomy. *Earth Planet. Sci. Lett.* 511, 44–54.
- Neumann, W., Henke, S., Breuer, D., Gail, H.-P., Schwarz, W.H., Trieloff, M., Hopp, J., Spohn, T., 2019. Modeling the evolution of the parent body of acapulcoites and lodranites: a case study for partially differentiated asteroids. *Icarus* 311, 146–169.
- Ormel, C.W., Klahr, H.H., 2010. The effect of gas drag on the growth of protoplanets. Analytical expressions for the accretion of small bodies in laminar disks. *Astron. Astrophys.* 520, A43.
- Pape, J., Mezger, K., Bouvier, A.-S., Baumgartner, L.P., 2019. Time and duration of chondrule formation: constraints from ^{26}Al - ^{26}Mg ages of individual chondrules. *Geochim. Cosmochim. Acta* 244, 416–436.
- Raymond, S.N., Izidoro, A., 2017. Origin of water in the inner solar system: planetesimals scattered inward during Jupiter and Saturn's rapid gas accretion. *Icarus* 297, 134–148.
- Reisberg, L., Dauphas, N., Lugué, A., Pearson, D.G., Gallino, R., Zimmermann, C., 2009. Nucleosynthetic osmium isotope anomalies in acid leachates of the Murchison meteorite. *Earth Planet. Sci. Lett.* 277, 334–344.
- Render, J., Fischer-Gödde, M., Burkhardt, C., Kleine, T., 2017. The cosmic molybdenum-neodymium isotope correlation and the building material of the Earth. *Geochem. Perspect. Lett.* 3, 170–178.
- Render, J., Brenneka, G.A., 2021. Isotopic signatures as tools to reconstruct the primordial architecture of the solar system. *Earth Planet. Sci. Lett.* 555, 116705.
- Savage, P., Moynier, F., Boyet, M., 2022. Zinc isotope anomalies in primitive meteorites identify the outer solar system as an important source of Earth's volatile inventory. *Icarus* 386, 115172.
- Schiller, M., Paton, C., Bizzarro, M., 2015. Evidence for nucleosynthetic enrichment of the protosolar molecular cloud core by multiple supernova events. *Geochim. Cosmochim. Acta* 149, 88–102.
- Schiller, M., Bizzarro, M., Fernandes, V.A., 2018. Isotopic evolution of the protoplanetary disk and the building blocks of Earth and Moon. *Nature* 555, 507–510.
- Schiller, M., Bizzarro, M., Siebert, J., 2020. Iron isotope evidence for very rapid accretion and differentiation of the proto-Earth. *Sci. Adv.* 6, eaay7604.
- Schönbächler, M., Rehkämper, M., Fehr, M.A., Halliday, A.N., Hattendorf, B., Günther, D., 2005. Nucleosynthetic zirconium isotope anomalies in acid leachates of carbonaceous chondrites. *Geochim. Cosmochim. Acta* 69, 5113–5122.
- Shollenberger, Q.R., Wittke, A., Render, J., Mane, P., Schuth, S., Weyer, S., Gussone, N., Wadhwa, M., Brenneka, G.A., 2019. Combined mass-dependent and nucleosynthetic isotope variations in refractory inclusions and their mineral separates to determine their original Fe isotope compositions. *Geochim. Cosmochim. Acta* 263, 215–234.
- Spitzer, F., Burkhardt, C., Budde, G., Kruijjer, T.S., Morbidelli, A., Kleine, T., 2020. Isotopic evolution of the inner solar system inferred from molybdenum isotopes in meteorites. *Astrophys. J.* 898, L2.
- Steele, R.C.J., Coath, C.D., Regelous, M., Russel, S., Elliott, T., 2012. Neutron-poor isotope anomalies in meteorites. *Astrophys. J.* 758, 59–79.
- Steller, t., Burkhardt, C., Yang, C., Kleine, T., 2022. Nucleosynthetic zinc isotope anomalies reveal a dual origin of terrestrial volatiles. *Icarus* 386, 115171.
- Sugiura, N., Fujiya, W., 2014. Correlated accretion ages and $\epsilon^{54}\text{Cr}$ of meteorite parent bodies and the evolution of the solar nebula. *Meteorit. Planet. Sci.* 49, 772–787.
- Torrano, Z.A., Brenneka, G.A., Williams, C.D., Romaniello, S.J., Rai, V.K., Hines, R.R., Wadhwa, M., 2019. Titanium isotope signatures of calcium-aluminum-rich inclusions from CV and CK chondrites: implications for early solar system reservoirs and mixing. *Geochim. Cosmochim. Acta* 263, 13–30.
- Touboul, M., Kleine, T., Bourdon, B., Van Orman, J.A., Maden, C., Zipfel, J., 2009. Hf–W thermochronometry: II. Accretion and thermal history of the acapulcoite-lodranite parent body. *Earth Planet. Sci. Lett.* 284, 168–178.
- Trieloff, M., Hopp, J., Gail, H.-P., 2022. Evolution of the parent body of enstatite (EL) chondrites. *Icarus* 373, 114762.
- Trinquier, A., Birck, J.-L., Allègre, C.J., 2007. Widespread ^{54}Cr heterogeneity in the inner solar system. *Astrophys. J.* 655, 1179–1185.
- Trinquier, A., Elliott, T., Ulfbeck, D., Coath, C., Krot, A.N., Bizzarro, M., 2009. Origin of nucleosynthetic isotope heterogeneity in the solar protoplanetary disk. *Science* 324, 374–376.
- Warren, P.H., 2011. Stable-isotopic anomalies and the accretionary assemblage of the Earth and Mars: a subordinate role for carbonaceous chondrites. *Earth Planet. Sci. Lett.* 311, 93–100.
- Yamakawa, A., Yamashita, K., Makishima, A., Nakamura, E., 2010. Chromium isotope systematics of achondrites: chronology and isotopic heterogeneity of the inner solar system bodies. *Astrophys. J.* 720, 150–154.